MNE 15 (2022) 100140

Contents lists available at ScienceDirect

Micro and Nano Engineering

journal homepage: www.sciencedirect.com/journal/micro-and-nano-engineering

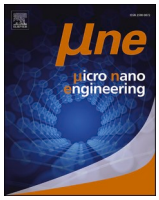

Textile-based pressure sensor arrays: A novel scalable manufacturing technique

Cagatay Gumus [a], Kadir Ozlem [b], Fidan Khalilbayli [b], Omur Fatmanur Erzurumluoglu [b], Gokhan Ince [b], Ozgur Atalay [a], Asli Tuncay Atalay [c,*]

[a] Faculty of Textile Technologies and Design, Istanbul Technical University, Istanbul 34437, Turkey
[b] Computer Engineering Department, Istanbul Technical University, Istanbul 34469, Turkey
[c] Faculty of Technology, Textile Engineering Department, Marmara University, Istanbul 34722, Turkey

ARTICLE INFO

Keywords:
Capacitive pressure sensors
Smart textiles
E-textiles
Textile-based sensors
Gesture recognition
Interactive devices

ABSTRACT

Soft pressure sensors have sparked a lot of interest over the last decade because of their applications in human motion recognition, object detection, and human–computer interaction. However, their mass production and availability to end users are limited due to the complex and time-consuming steps. The scalability of working range for various applications is also a critical challenge. Therefore, a laborless, rapid, and scalable manufacturing technique for capacitive-based soft pressure sensors with high sensitivity and high working range is proposed in this work. The novel manufacturing method enables manipulation of sensor properties by varying production parameters based on specific application needs. The proposed sensor's electrode is made of conductive knit fabric, and the dielectric layers are made of thermoplastic polyurethane (TPU) sheets. As a result of the novel approach, it is possible to generate scalable air gaps between electrodes and dielectric layers to capture low pressures of less than 1 kPa. The usage of multi-layer TPU sheets also increases the working range of sensors up to 1000 kPa. Here, the proposed technology is successfully applied to create several sensor mats for different purposes such as improved gesture and shape recognition, and interactive gaming mats for children.

1. Introduction

Over the past two decades, the development and investigation of electronic textile structures have received a lot of attention due to inherent softness, breathability, and flexibility. These characteristics create a satisfying platform to sense various stimuli such as strain, pressure, and temperature [1–3]. Textile-based sensors are able to distinguish a variety of stimuli simultaneously from the environment and can be used in a wide range of applications i.e., electronic skin [4,5], rehabilitation/personal healthcare [6,7], virtual reality (VR) and augmented reality (AR) applications [8,9], pressure mapping [10,11], and motion detection such as breathing, speaking, and joint movements [12–14].

According to the sensing mechanism, further classifications can be made between piezoresistive [15], capacitive [16,17], triboelectric [18], and also hybrid devices [19], demonstrating the relevance and diversity of the sensor researches. When it comes to the application of strain and pressure sensors in real-world circumstances, various indicators can be used to assess the performance of these sensors, including stretchability, sensitivity, mechanical durability as well as response time [20,21]. Among the various sensor types, capacitive sensors are appealing because of their advantages, including their simple structure, low power consumption, quick response, signal repeatability, and so on [22].

Capacitive pressure sensors are parallel plate capacitors with a dielectric sheet placed between two flexible electrodes. Capacitive pressure sensors detect changes in capacitance as a result of applied pressure and convert those changes into electrical signals. The following equation defines the capacitance.

$$C = \varepsilon_0 \varepsilon_r \frac{S}{\delta}, \tag{1}$$

where the capacitance C is determined by the parameters: ε_0 corresponds to the free space permittivity, ε_r is the relative permittivity, S is the area of the conductive plates and δ is the distance between the plates [22,23].

* Corresponding author.
E-mail address: asli.atalay@marmara.edu.tr (A.T. Atalay).

https://doi.org/10.1016/j.mne.2022.100140
Received 28 February 2022; Received in revised form 1 April 2022; Accepted 9 April 2022
Available online 18 April 2022

Many researches have been conducted to manufacture pressure sensors so far. For example, in order to overcome the sensitivity and sensing range limitations of pressure sensors, Yang et al. [24] created a solution based on polyvinylidene fluoride (PVDF) powder and carbon nanotubes that is used in the electrospinning process to create a nanofiber dielectric layer. Indium tin oxide polyethylene terephthalate films are preplaced to the surfaces of the nanofiber dielectric layer as electrodes. Vu et al. [25] used SWCNT ink and stretchable silver paste to create electrode patterns on polyester/spandex (PET/SP) fabrics in another study. Screen printing was used to print single-walled carbon nanotubes (SWCNTs) on the top and bottom sides of the spacer fabric. Following that, the sensors are shaped by a laser cutting, and the encapsulation pastes are injected into the spacer layer. At the end of this step, capacitive pressure sensors with Ag/SWCNT electrode layers were formed.

Lee et al. [26] proposed a method to fabricate capacitive air-gap touch sensors via printing and coating. The bottom electrode was first printed on a PET substrate with silver ink using roll-to-roll gravure printing. Then, using a polyimide (PI) pattern mask, PDMS was mixed with a curing agent and spin-coated to form a sacrificial layer. The top electrode was created by spin coating a stretchable silver ink onto the sacrificial layer. The sensor samples were then immersed in a tetrabutylammonium (TBAF) bath to remove the sacrificial layer and create an air gap. Another advancement was reported by Atalay et al. [27] who proposed a way to increase the sensor sensitivity by generating micropores in the dielectric layer. Towards this aim, silicone elastomer and sugar granules were mixed and cured, then the granules were dissolved in an ultrasonic washing tank, leaving micropores in the silicone elastomers. The electric layer is sandwiched between two conductive fabrics at the end.

A capacitive sensor enhanced by a tilted micropillar array-structured dielectric layer is developed by Luo et al. [28]. In this work, photoresist was spin coated on a silicon wafer and exposed to UV light to create the template. Following that, poly-(dimethylsiloxane) (PDMS) was poured and cured to create a dielectric layer structure with tilted micropillar arrays, which was then bonded to Au-coated PET electrodes. Pyo et al. [29] present a capacitive tactile sensor comprised of graphene electrodes that are separated by spacers which form air gaps. Chemical vapor deposition was used to create monolayer graphene, which was then transferred to PET substrates. Electrodes patterned by photolithography and etched by O2 plasma. For spacer fabrication, photolithography was used to pattern SU-8 on the PET film. In the meantime, PDMS was spin-coated on the other graphene and exposed to N2 plasma to form amino groups capable of reacting and bonding with epoxy groups on the SU-8 surface. Finally, the top and bottom layers were aligned and bonded together. Furthermore, a multimaterial 3D printing technology was utilized to produce a tactile sensing mechanism that have a specific geometry to fit the curved surfaces by Guo et al. [30] Using Ag/silicone ink, the bottom electrode layer was printed on the silicon base layer. The silicone and pluronic inks were used to print the isolating and supporting layers, respectively, and the top electrode was printed on the supporting layer to create the sensor.

Despite the advancements in soft pressure sensor technologies, there are still significant manufacturing complexity that limits the scalability of sensors in terms of high sensitivity, high resolution, quick response, good stability, and durability over the various applications [31]. Here, a novel pressure sensor arrays fabrication technique will be described in order to meet the demand for a scalable, laborless, rapid, and repeatable fabrication strategy for mass production and commercialization. The developed manufacturing method is adequate for large-scale production and the proposed pressure-sensing mattresses have the ability to detect pressures over a broad working range (0 kPa - 445 kPa for 10×10 mm^2 cell, 0 kPa - 1000 kPa for 15×15 mm^2) cell, making them very competitive among the other products in the market.

2. Experimental section

In this paper, we overcome above mentioned difficulties by proposing an effective and simple novel manufacturing method for textile-based capacitive pressure sensors fabricated with conductive fabric electrodes and dielectric TPU (Fibre Glast Developments Corp - Stretchlon 200 Bagging Film) layers. In order to achieve high sensitivity, we used a novel technique to generate air gaps within the sensor itself, and we also alternated sensor properties (sensitivity, working range, and response/recovery time) by modifying manufacturing parameters, resulting in versatility for various application areas. While the presence of air gaps significantly enhances sensitivity, the dielectric layers maintain the integrity of the produced sensor arrays and determine their operating range. This strategy is essential for real-world applications that require highly sensitive and robust pressure sensors.

In order to adjust the capabilities of pressure sensors, it is important to understand the effect of dielectric layers and sensor array cell sizes on sensitivity and working range. For this aim, we also investigated the contribution of number of different TPU layers (1, 2, and 3 layers) on the working range of the pressure sensors and formed two different cell sizes (10 and 15 mm side length) to observe air gaps formation within the sensor cells to better understand how air gaps affect sensor sensitivity.

We found that adding extra TPU layers increases the working range of sensors whereas the sensor arrays that have bigger air gap (AG) / cell size (CS) ratio yielded higher sensitivity, which can be explained by the amount of air gap and lower stiffness. On the other hand, the sensor density of pressure mats is dependent on cell size and proximity of each cell, therefore utilizing smaller cell sizes provided the best object resolution, as expected.

Our novel manufacturing technique can be divided into four main steps: (1) laser cutting of the conductive knitted fabric (Shieldex Med-Tex P130, thickness of 0.45 mm $\pm$ 10%) as upper and lower electrode layers, (2) the formation of square cells in a double-sided fusible sheet (Can-Do National Tape - Custom Converted Clear Thermoplastic Polyurethane Sewfree Tape) using laser cutting, (3) generating cavities in the pressure plate (Plexiglass/Acrylic (PMMA), thickness of 4 mm) that are consistent with the cell dimensions from the previous stage, and (4) replacing dielectric (TPU) layers between electrodes and applying heat at 90 °C for 5 s to all sensor layers that are stacked over the designed pressure plate. The unique production approach for textile based capacitive pressure sensors is shown in Fig. 1.

Fig. 1(a) demonstrates the shaping of conductive knitted fabric into sensor arrays with desired dimensions for end-use applications, as well as an optical microscopy image of the loops in the knitted fabric. Following that, creating square spaces via laser cutting in the double-sided fusible sheets which is responsible for keeping electrode and dielectric layers together. It should be noted here that creating cells in the fusible sheet has a direct impact on the amount of air gap formation in the manufactured pressure sensors therefore it ought to be carefully adjusted in terms of dimensions.

The stacking sequence of all the sensor layers is shown in Fig. 1(b), with upper and lower conductive knitted fabrics acting as electrodes, TPU layers between them acting as dielectric layers, and double-sided fusible sheets bonding all together. The image also illustrates the application of heat and pressure to the layers that are replaced one by one over the pressure plate by the heat press (Serfo - Automatic Transfer Printing Press). The importance of the pressure plate here is that it is positioned beneath the layers during the manufacturing process, and when heat is applied from the top to melt the fusible layers, the edge points of the arrays are determined by the cavities of the plate, so that the pressure is only applied to the edges of the arrays, and the knit fabric begins to widen through these holes, generating air gaps.

After all, as shown in Fig. 1(c), the textile-based pressure mat has been obtained in the desired shape and size, following the application of heat and pressure (see also Movie S1, Supporting Information). The real images of pressure sensor arrays along with air gaps in each cell can be

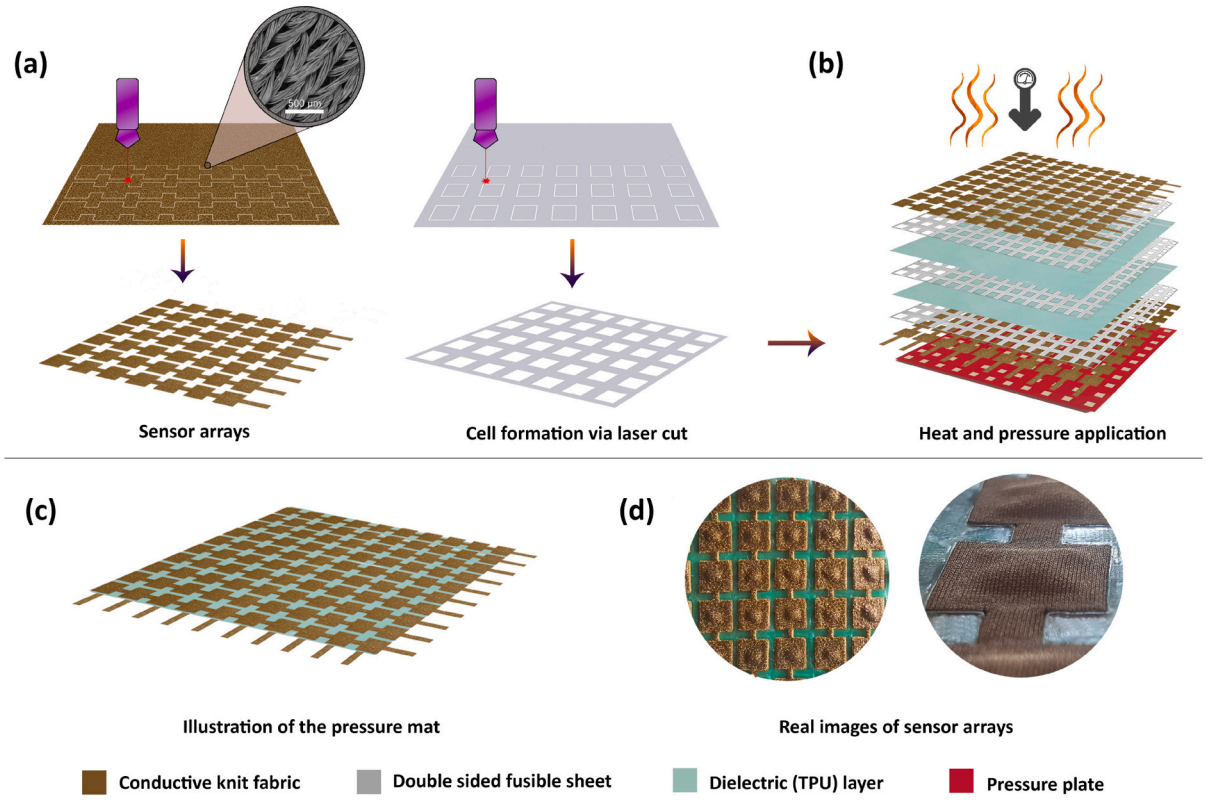

Fig. 1. Schematic diagram of the fabrication process of the textile-based capacitive pressure sensor. (a) Laser cutting of conductive knitted fabric into sensor arrays and the creation of square cells in a double-sided fusible sheet. (b) Replacement of dielectric (TPU) layers between electrodes and application of heat to all sensor layers stacked over the designed pressure plate. (c) Illustration of fabricated the textile-based pressure mat. (d) Actual images of pressure sensor arrays having air gaps in each cell.

seen in Fig. 1(d). The elimination of complex fabrication steps to enable mass production, as well as the controllability of sensor characteristics in terms of working range and sensitivity by adding extra dielectric layers and altering air gap formation are inherent advantages of this manufacturing approach.

3. Characterization results

3.1. Manufactured specimens and macrostructure

In order to scrutinize the efficiency of sensor cells as well as demonstrate the scalability of the manufacturing approach, 9 pieces of 10 × 10 mm^2, and 9 pieces of 15 × 15 mm^2 pressure sensor cells were produced utilizing the introduced manufacturing process. The electrode dimensions, number of dielectric sheets, and air gaps within the sensor cells were modified during the study to alternate the sensitivity, durability, working range, and stability performance for identification of optimum sensors in various fields of application. During the study, three experimental setups were designed to examine the sensitivity, durability, working range, and stability performance of samples (more details can be seen in Figs. S1–3, Supporting Information). The photographs and microscopic images are illustrated in Fig. 2 to demonstrate the prepared 15 × 15 mm^2 sensors that are designed with increasing numbers of dielectric layers for the further characterization stages. Fig. 2(a) represents the pressure sensor cells that are devoid of air gaps to truly comprehend how air gaps influence the sensor performance, while Fig. 2(b) and (c) show the sensor cells with varying amounts of air gaps as an outcome of modifying pressure plate cavities and changing fusible layer dimensions, demonstrating the scalability of the developed technique. The cross-sectional microscopic images of 10 × 10 mm^2 sensor cells are shown in the Supporting Information (Fig. S4).

3.2. Sensitivity characterization

The sensing capabilities of the capacitive pressure sensors are assessed as shown in Fig. 3. To determine the scalability of manufacturing procedure, the above mentioned 15 × 15 mm^2 and 10 × 10 mm^2 sensor cells with varying air gaps and TPU layers were tested and compared to sensors with no air gap by using the experimental setup which is developed for the sensitivity characterization (see Fig. S1, Supporting Information). Fig. 3(a-c) represent the sensing behavior of 15 × 15 mm^2 sensor cells with increasing numbers of dielectric TPU layer. The pressure sensitivity of the fabricated sensor cells increases as the air gap amount increases from 0 to 44%, according to the results of the sensitivity characterization. The sensor with the highest amount of air gap and the thinnest dielectric layer as in see Fig. 3(a) had best sensitivity with 306.69 × 10^{-2} kPa^{-1} (below 1 kPa) and 9.44 × 10^{-2} kPa^{-1} (between 1 kPa and 30 kPa). This is then followed by the sensor of 11% in terms of AG/CS ratio which has lower amount of air gap, with the sensitivities of 110.79 × 10^{-2} kPa^{-1} and 2.76 × 10^{-2} kPa^{-1}, respectively. Moreover, the sensor that has no air gap showed the least sensitivity performance while proving the efficiency of our approach (see Table S1, Supporting Information).

On the other hand, 10 × 10 mm^2 sensor cells performed higher sensitivity compared to 15 × 15 mm^2 cells, due to the higher air gap/cell size ratio of 10 × 10 mm^2 sensors. Similar to the previous sensitivity tests, Fig. 3(d-f) show the sensitivity characteristics of 10 × 10 mm^2 sensors, with a similar increase depending on the amount of air gap. Among these sensors, the sensor 56% which has a single layer of TPU and highest amount of air gap exhibited the best sensitivity 268.82 × 10^{-2} kPa^{-1} (below 1 kPa) and 6.36 × 10^{-2} kPa^{-1} (between 1 kPa and

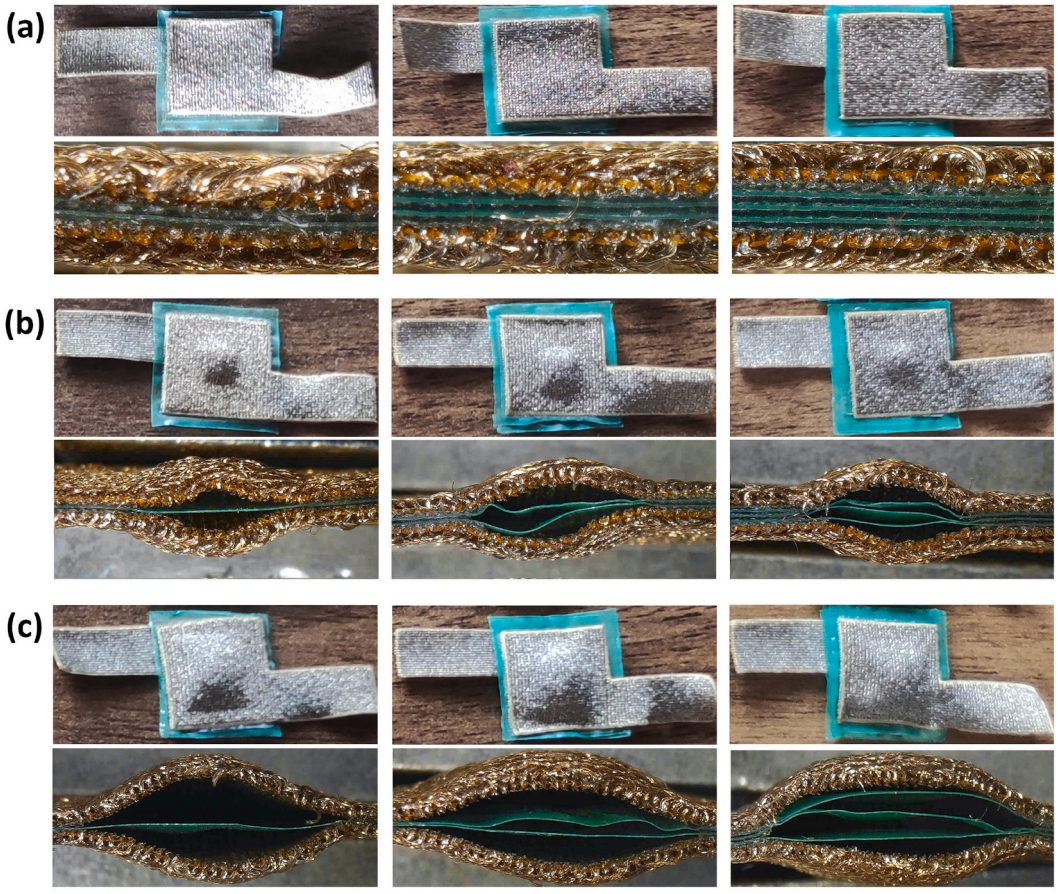

Fig. 2. Optical and cross-sectional microscopic images of 15 × 15 mm^2 textile-based capacitive sensor specimens with one, two, and three dielectric TPU layers from left to right. (a) Sensor cells with no air gaps. (b-c) Air-gapped sensor cells manufactured by utilizing pressure plates with a cavity of 5 × 5 mm and 10 × 10 mm^2, respectively. These two air-gapped sensors are named as "11%" and "44%" due to their air gap/cell size (AG/CS) ratio.

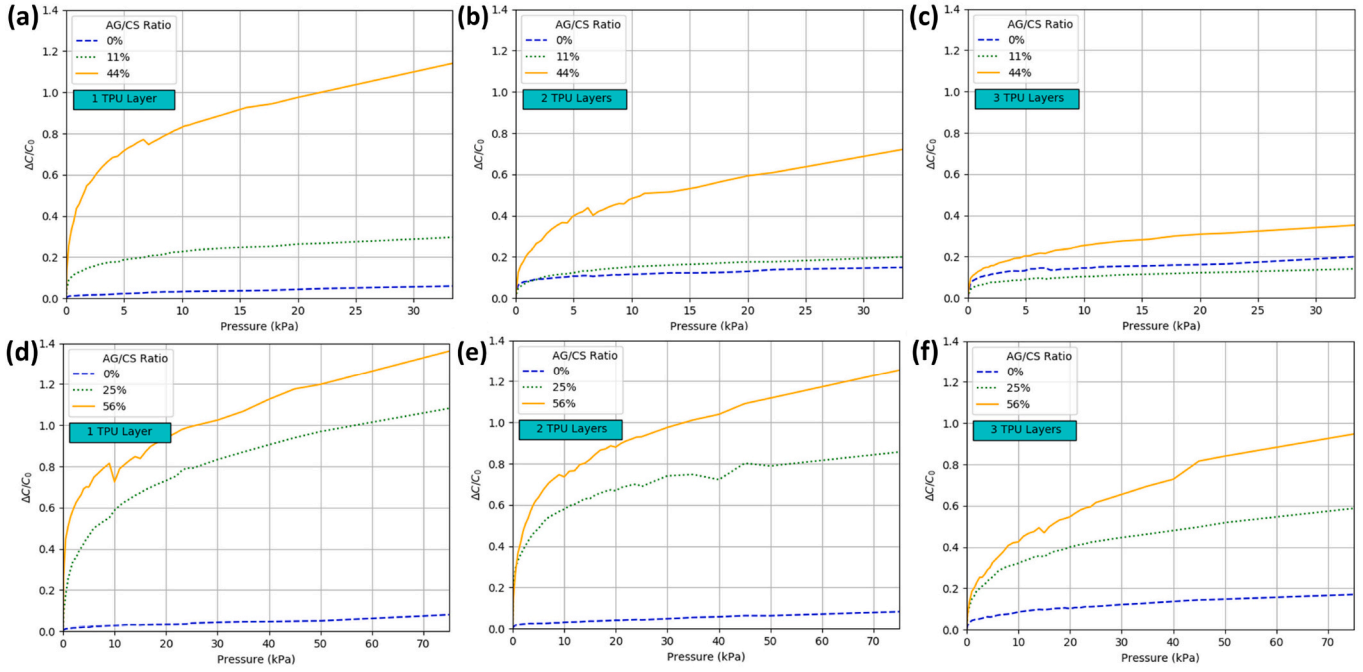

Fig. 3. Sensitivity results of the square sensor cell specimens with one, two, and three dielectric TPU layers from left to right. (a-c) The sensitivity values of 15 × 15 mm^{-2} pressure censor cells. (d-f) The sensitivity values of 10 × 10 mm^{-2} sensor cells. Different colors represent the different AG/CS ratios within sensor cells that are generated by the pressure plate cell cavities and fusible layer cells depending on the dimensions.

30 kPa). This followed by the sensor 25% which has relatively low amount of air gap, with the sensitivities of 86.09 × 10^{-2} kPa^{-1} and 7.55 × 10^{-2} kPa^{-1}. In terms of TPU layer comparison, due to dielectric thickness, sensors with single layers performed highest sensitivity, and followed by sensors that has 2 and 3 TPU layers, respectively. This demonstrates that, dielectric thickness has a negative impact on sensor sensitivities as expected (see Table S1, Supporting Information).

3.3. Analysis of response and recovery time

Response and recovery durations of pressure sensors are also important parameters to consider when minimizing the delays in applications, therefore response and recovery time of the sensor cells with different sizes and air gaps were analyzed. We first tested 15 × 15 mm^2 sensors with one layer of dielectric TPU to determine the effect of air gap on response time of the proposed sensors. The tests for the electrical response were carried out by putting 100 g weight (corresponding to 4.35 kPa) on the sensors and the sensor without air gap shows a response time of 140 ms and a recovery time of 360 ms (Fig. 4(a)). On the contrary, the response time was measured to be only 160 ms and a recovery time of 7.32 s for the sensor with 44% air gap (Fig. 4(b)).

The results of 10 × 10 mm^2 sensors tested with 50 g weight (4.9 kPa) are shown in Fig. 4(c) and Fig. 4(d). The sensor without air gaps has a response/recovery time of 140 ms and 240 ms, whereas the sensor with air gaps, similar to the previous sensors, has a response time of 220 ms and a long recovery time of 7 s, respectively. The results reveal that the recovery time of an air-gapped sensor is longer than that of a non-air gapped sensor. The difference in recovery times can be ascribed to the fact that the relaxation time of conductive knit fabric takes a long time after unloading the weight.

3.4. Characterizations of durability and working range

The mechanical durability of the capacitive pressure sensors in terms of pressure sensitivity is tested by subjecting the 10 × 10 mm^2 cells and 15 × 15 mm^2 cells to 1000 cycles of loading/unloading pressure of 50 and 22.2 kPa, respectively at a speed of 20 mm/s. For more details about testing and designed cycle test set-up, see Fig. S2, Supporting Information. Following the sensitivity results, the best performing air-gapped sensors and air gap-free sensors are chosen for comparison in the cycle test. By comparing the initial and last cycles of air-gapped 15 × 15 mm^2 sensors (Fig. 5(a)) and air-gapped 10 × 10 mm^2 sensors (Figure(b)), we observed that electrical performance of 15 × 15 mm^2 sensors show less than 6.32% and 10 × 10 mm^2 sensor show less than 4.47% variation over the 1000 cycles, demonstrating that the performance of manufactured pressure sensor is consistent for long-term use. However, the sensors that are devoid of air gaps exhibit relatively lower degradation less than 1.83%, due to the robustness of sensors without air gaps (see Fig. S5, Supporting Information).

Fig. 5(c) and (d) illustrate the sensitivity change of the sensors under a constant load 100, 250, and 500 g of weight (approx. 4.35, 10.9 and 21.8 kPa for 15 × 15 mm^2 sensor and 9.8, 24.5 and 49 kPa for 10 × 10 mm^2 sensor cell) for 1 h. As shown, when a constant pressure was applied to the sensor cells, the capacitance abruptly increased within milliseconds, then reached a plateau and no other significant capacitance chance has been observed during the period of 1 h. This property has demonstrated that the proposed sensors are durable for constant pressure and are suitable for applications that require long-term stability, such as shoe insoles, wheelchairs, or smart beds. Furthermore, in order to meet the practical engineering application, it was necessary to investigate the effect of dielectric thickness on the developed sensors'

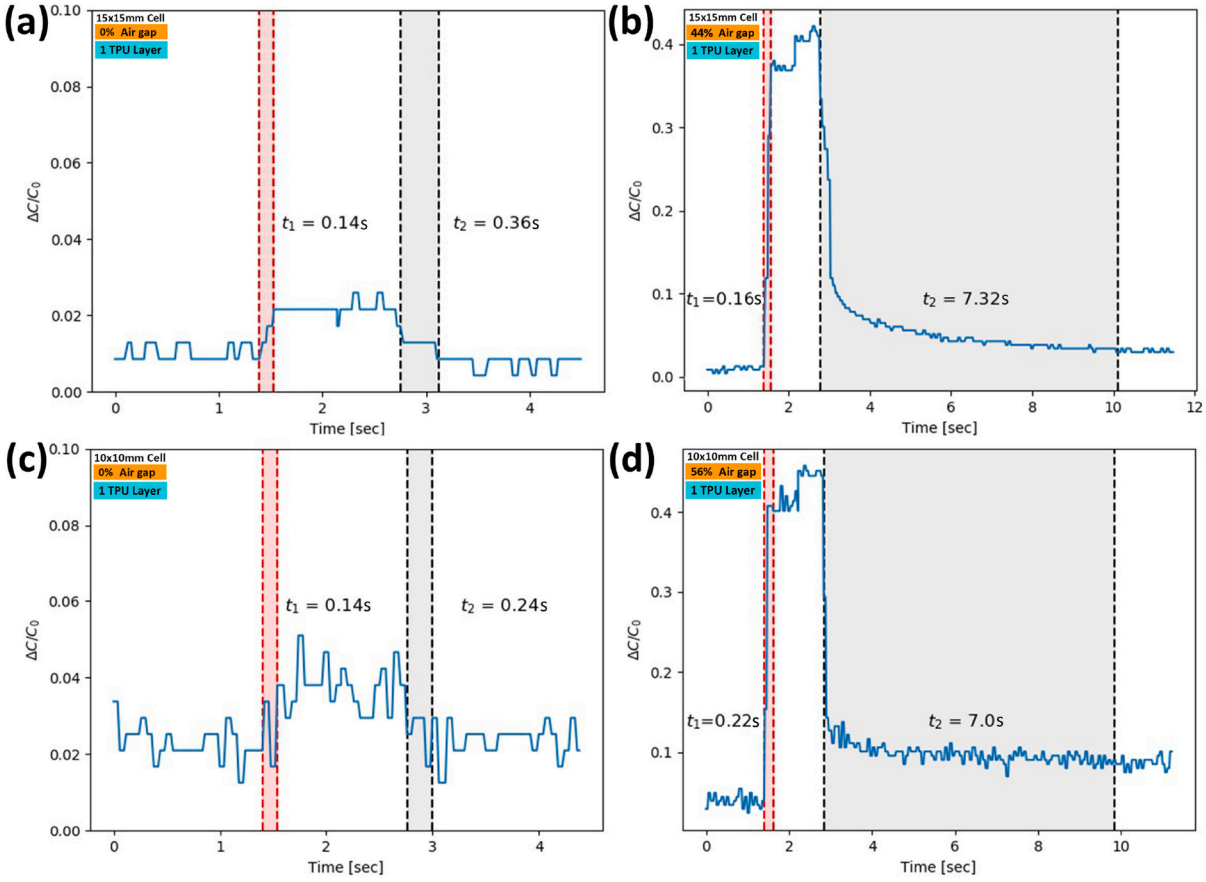

Fig. 4. Response and recovery times of the proposed pressure sensors. (a,b) Performance of the 15 × 15 mm^2 non-airgapped and air-gapped pressure sensors with loading-unloading of 100 g (4.35 kPa) weight. (c,d) Performance of the 10 × 10 mm^2 non-airgapped and air-gapped pressure sensors using 50 g (4.9 kPa) weight.

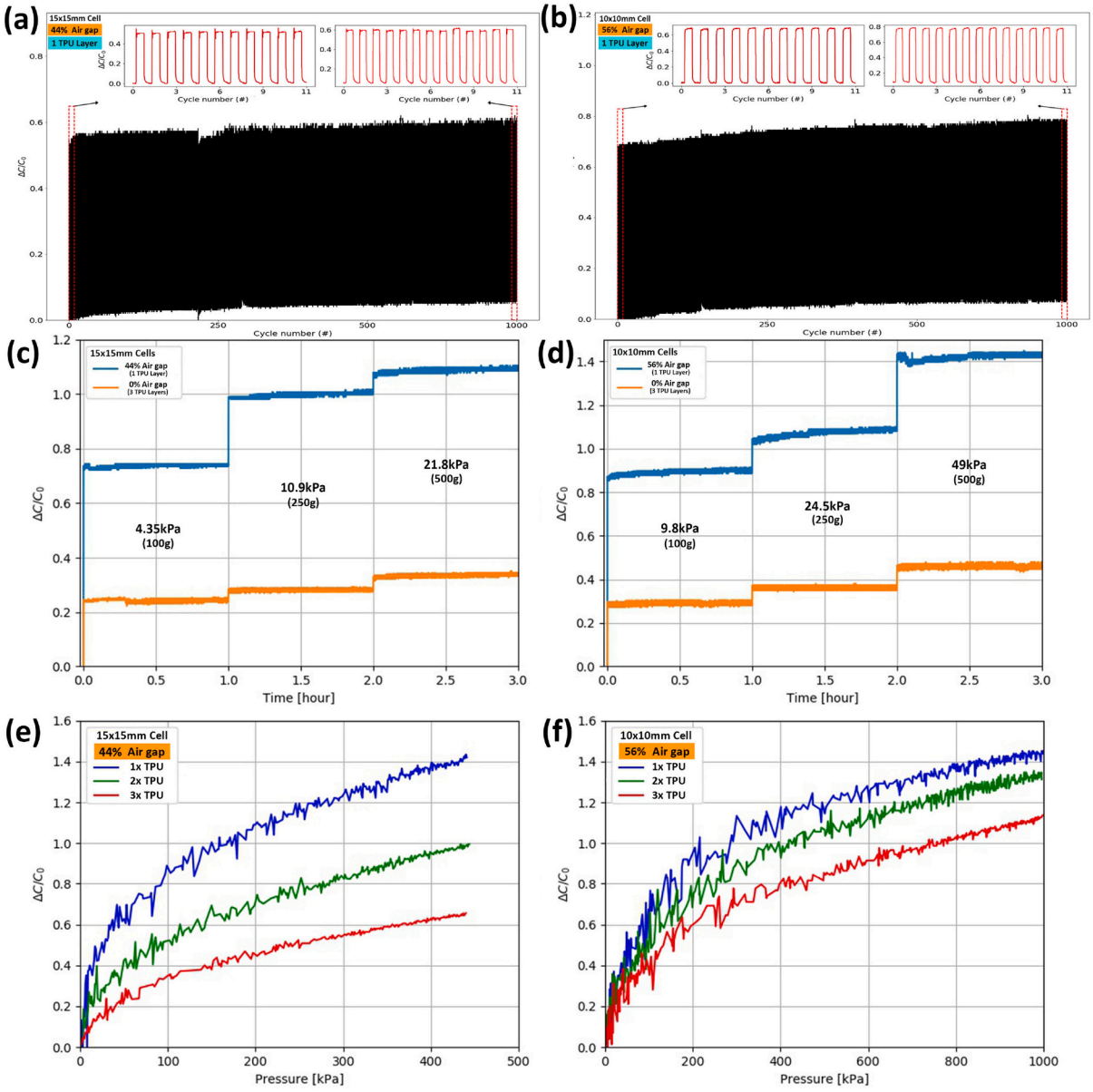

Fig. 5. Durability and working range test results of the most sensitive sensor specimens. (a,b) Capacitance changes of the 15 × 15 mm^2 and 10 × 10 mm^2 sensor cells when subjected to a pressure of 22.2 and 50 kPa, respectively under 1000 repeated cycles. Constant weight performance of 15 × 15 mm^2 (c) and 10 × 10 mm^2 (d) sensor cell specimens under 100, 250, and 500 g for 1 h. (e,f) Working ranges of 15 × 15 mm^2 and 10 × 10 mm^2 sensors with varying numbers of dielectric TPU layers.

sensing range and sensitivity. The detection limit of the sensors was demonstrated by applying pressure to the sensor over a wide range of pressures ranging from 1 to 1000 kPa. Fig. 5(e) depicts the responses of a 15 × 15 mm^2 air-gapped sensor with varying numbers of dielectric TPU when pressure is applied (measured up to 435 kPa), and Fig. 5(f) depicts the capacitance change of a 10 × 10 mm^2 sensor when pressure is applied (measured up to 1 MPa) via the developed test set up in Fig. S3, Supporting Information. The result reveals a detection limit of less than 1 kPa, indicating that the sensor's performance is only valid within a relatively narrow pressure range; in our case, the sensor remains sensitive at pressures up to 1 MPa. It is expected that the sensitivity and detection range can be customized by adjusting structural parameters such as electrode size, air gap amount, and number of dielectric layers.

4. Applications

4.1. Object recognition

The developed pressure sensor mats are utilized in object recognition system (Fig. 6). The system can differentiate objects placed on the mats and determine their respective locations on the mats using their shape and weight information. Since the manufactured mats are capable of measuring the applied pressure level in each cell, the heatmap of the placed object is visualized using the python Tkinter module [32]. Then the created heatmaps are processed as an binary image and the object recognition is carried out on the obtained images by using Connected-component analysis which labels the different regions that correspond to different objects on the image (see Movie S2, supporting Information). The regions are labelled according to their pixel intensity values. After identifying the shape of the object, its weight was determined by

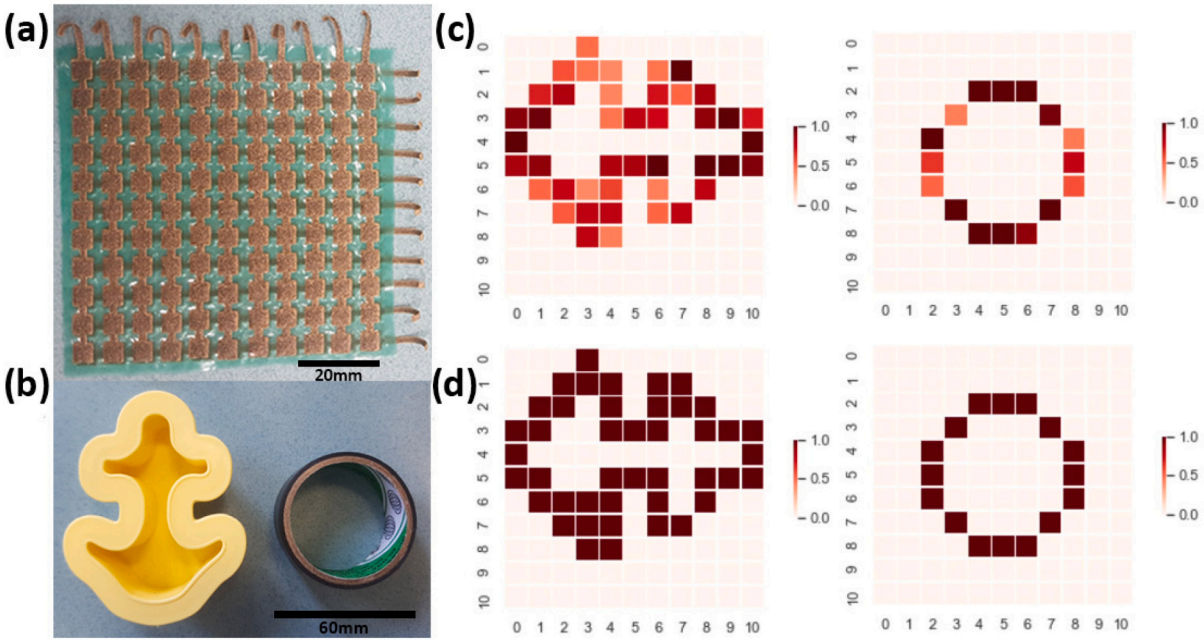

Fig. 6. Object Recognition System. (a) Fabricated pressure mat with 11 × 11 sensor arrays. (b) The objects that were used to apply pressure. (c-d) Heatmap visualization of objects over the textile-based pressure mat.

thresholding the individual cell values. To better analyze the performance of the developed object recognition system, various objects with different weights and shapes were tested.

4.2. Gesture detection and recognition

Another application for the manufactured mat is based on gesture detection and recognition from the capacitive sensor array as shown in Fig. 7. After the data is collected from the mat, a low pass filter is applied to the data. To find a base signal level for a cell while being in stable condition, an automatic calibration system is developed. Then, a threshold value is set for activation of each cell. A boolean map of the mat is obtained which can be used as an input for gesture detection (see Movie S2, supporting Information).

A consequent gesture recognition works by finding each cluster of presses in each frame and connecting them to the closest cluster in the previous frame; if none is found in a sufficiently large area a new cluster label is added. Each trace is first filtered using Kalman Filter and then processed to fit the closest described gesture. The result of processed path input obtained from the developed mat is shown in Fig. 7(a) as a circle, and Fig. 7(b) as a double line. Here, the user traces the mat simply with the fingers, and the trace along with its detected gesture is shown

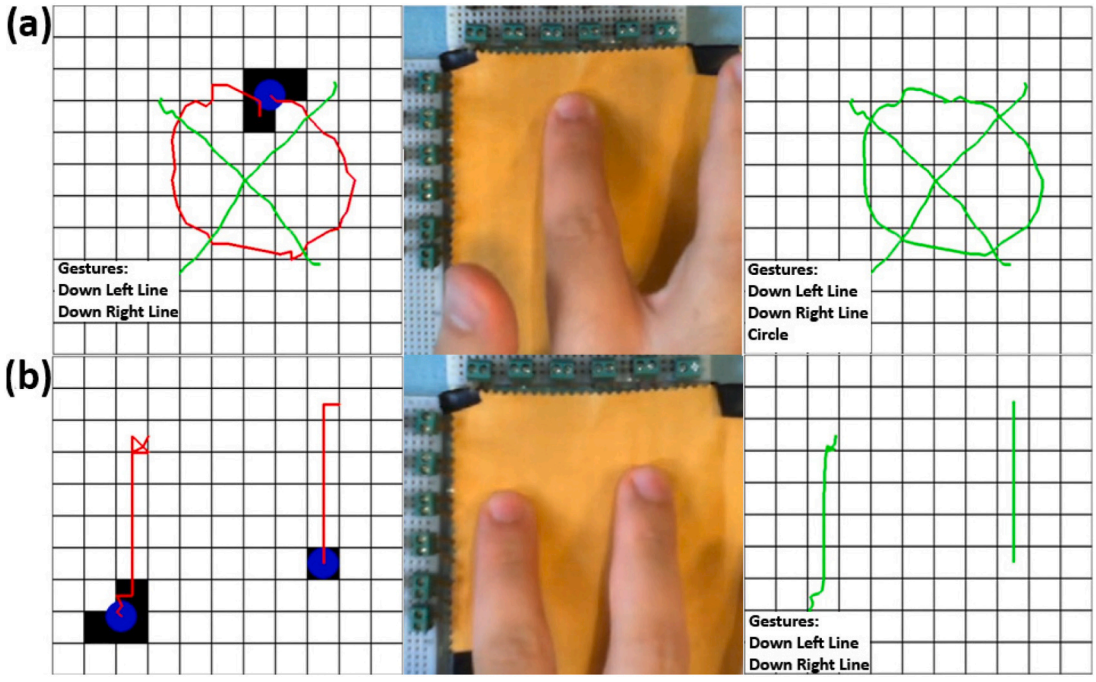

Fig. 7. Textile-based pressure sensing system and gesture examples. (a) Circle trace gesture recognition. (b) Double line trace gesture recognition.

on the computer.

4.3. Tangible interaction gaming platform for children

Game-based learning has received a tremendous research interest in modern education. One of the most prominent benefits of this sort of learning is the connection to the virtual world. In this application, a sensor mat is utilized as a tangible interaction platform that can provide both visual and audio feedback to the user. The tangible user interface is integrated with devices such as phones that realizes the functionality of the mat without needing any extra screens. The developed mat is connected to Arduino, which transfers the sensor value of each cell to the Android phone over Bluetooth using a HC-06 serial module. Several Android mobile applications focusing on Math and Alphabet Game are developed which utilize the produced mat as a playground for the children as shown in Fig. 8(a) and Fig. 8(b) respectively. For each application, a distinct cover which constitutes of different button positions, toy areas, etc. are produced and positioned on top of the mat.

The Math game in Fig. 8(a) is developed for children of the age range 4 to 8. In this game, several interfaces are created. The first game mode enables the user to press any of the numbers on the mat which subsequently returns the pronunciation of the number from the phone. The second mode, on the other hand, asks the user to press the number shown in the quiz application on the phone. The third game mode provides several objects on the phone and asks the user to enter the number of the objects on the mat. The fourth game mode is developed for older children as it requires the child to enter the result of the equation on the mat (shown in Movie S2, Supporting Information).

The Alphabet Game in Fig. 8(b) is designed for children between the age of 4 and 7. This game has 4 modes that can be chosen from the mat. In the first mode, the child presses any letter on the mat which returns the written and audio version of the letter in the display of the phone. The second mode operates in the same manner, but here the child learns the same word starting with the corresponding initial letter. The third and the fourth mode tests the child using the letters learned in the former modes. Here, the child is requested to press the respective letter/object shown on the screen of the phone on the mat buttons.

5. Conclusion

In summary, we have proposed a novel textile-based pressure sensor fabrication technique for eliminating complex and time-consuming manufacturing conditions and creating sensors with desired patterns and steady characteristics. Different types of sensor cells with variable air gaps and TPU (dielectric) layers were initially created using a combination of stacking laser cut layers and a pressure plate assisted heat application technique to assess the potential application fields for each type of sensor. Afterwards, the sensors produced during the research were experimentally tested and observed to have a high and adjustable sensitivity as well as a wide working range, displaying the effectiveness of our approach. We have shown that a device sensitivity of as high as of 306.69×10^{-2} kPa^{-1} within the pressure range of 0–1 kPa and 9.44×10^{-2} kPa^{-1} for 1–30 kPa, detection range up to 1000 kPa, stable cycling performances (up to 1000 cycles), a fast response time (≈140 ms), and mechanical stability under constant deformations are achieved. Thanks to these features, our sensors are ideal candidates for effective integration with other functional devices such as e-textiles, wearable devices, and interactive software. We demonstrated the application of pressure sensor arrays for the recognition of various human gestures. Also, mechanical and computational tools enabled us to design educational mobile games, and tangible user interfaces to detect object shapes in high-resolution using pressure sensor mats. We believe that this cutting-edge manufacturing approach used to develop our sensor will meet the competitive market demands for textile-based sensor manufacturing, and opens new routes to fabricating sensors to be used in many fields such as wearable systems, rehabilitation, entertainment, and gaming.

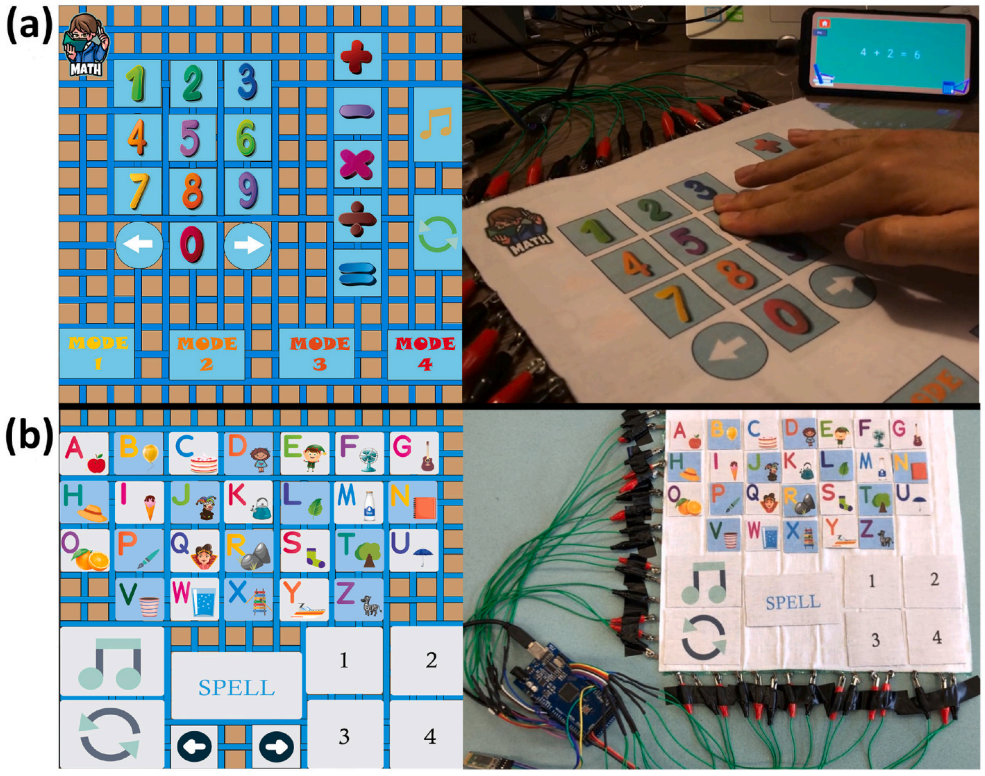

Fig. 8. Layout designs of tangible interaction mats on the left and the real world applications of mats on the right. (a) Math game platform. (b) Alphabet game platform.

Declaration of Competing Interest

The authors declare no conflict of interest.

Acknowledgements

This study was funded by the Scientific and Technological Research Council of Turkey (TÜBİTAK), Research Grant No:120C118. We thank Huseyin Özlem for his assistance in manufacturing of cycle test stand. We thank Erhan Önal, Cemalettin Cem Belentepe, Helga Lukaj, and Burak Akın for the development of applications. We also thank Soft Sensors Lab members for their assistance.

Appendix A. Supplementary data

Supporting Information is available from the Sensors and Actuators A: Physical Website or from the author.

References

[1] G.M.N. Islam, A. Ali, S. Collie, Textile sensors for wearable applications: a comprehensive review, Cellulose 27 (11) (2020) 6103–6131, https://doi.org/10.1007/s10570-020-03215-5.
[2] S. Liu, K. Ma, B. Yang, H. Li, X. Tao, Textile electronics for vr/ar applications, Adv. Funct. Mater. 2007254 (2020) 2007254, https://doi.org/10.1002/adfm.202007254.
[3] O. Atalay, F. Kalaoglu, S. Kursun Bahadir, Development of textile-based transmission lines using conductive yarns and ultrasonic welding technology for e-textile applications, J. Eng. Fibers Fabrics 14 (2019), https://doi.org/10.1177/1558925019856603, 155892501985660.
[4] X. You, J. He, N. Nan, X. Sun, K. Qi, Y. Zhou, W. Shao, F. Liu, S. Cui, Stretchable capacitive fabric electronic skin woven by electrospun nanofiber coated yarns for detecting tactile and multimodal mechanical stimuli, J. Mater. Chem. C 6 (47) (2018) 12981–12991, https://doi.org/10.1039/C8TC03631D.
[5] J. Zhang, L. Wan, Y. Gao, X. Fang, T. Lu, L. Pan, F. Xuan, Highly stretchable and self-healable mxene/polyvinyl alcohol hydrogel electrode for wearable capacitive electronic skin, Adv. Electr. Mater. 5 (7) (2019) 1900285, https://doi.org/10.1002/aelm.201900285.
[6] W. Fan, Q. He, K. Meng, X. Tan, Z. Zhou, G. Zhang, J. Yang, Z.L. Wang, Machine-knitted washable sensor array textile for precise epidermal physiological signal monitoring, science, Advances 6 (11) (2020) eaay2840, https://doi.org/10.1126/sciadv.aay2840.
[7] F. Porciuncula, A.V. Roto, D. Kumar, I. Davis, S. Roy, C.J. Walsh, L.N. Awad, Wearable movement sensors for rehabilitation: a focused review of technological and clinical advances, PM&R 10 (9S2) (2018) S220–S232, https://doi.org/10.1016/j.pmrj.2018.06.013.
[8] F. Wen, Z. Sun, T. He, Q. Shi, M. Zhu, Z. Zhang, L. Li, T. Zhang, C. Lee, Machine learning glove using self-powered conductive superhydrophobic triboelectric textile for gesture recognition in vr/ar applications, Adv. Sci. 7 (14) (2020) 2000261, https://doi.org/10.1002/advs.202000261.
[9] O. Glauser, S. Wu, D. Panozzo, O. Hilliges, O. Sorkine-Hornung, Interactive hand pose estimation using a stretch-sensing soft glove, ACM Trans. Graph. 38 (4) (2019) 1–15, https://doi.org/10.1145/3306346.3322957.
[10] X. Wu, Y. Khan, J. Ting, J. Zhu, S. Ono, X. Zhang, S. Du, J.W. Evans, C. Lu, A. C. Arias, Large-area fabrication of high-performance flexible and wearable pressure sensors, Adv. Electr. Mater. 6 (2) (2020) 1901310, https://doi.org/10.1002/aelm.201901310.
[11] M. Liu, X. Pu, C. Jiang, T. Liu, X. Huang, L. Chen, C. Du, J. Sun, W. Hu, Z.L. Wang, Large-area all-textile pressure sensors for monitoring human motion and physiological signals, Adv. Mater. 29 (41) (2017) 1703700, https://doi.org/10.1002/adma.201703700.
[12] K. Ozlem, O. Atalay, A. Atalay, G. Ince, Textile based sensing system for lower limb motion monitoring, in: L. Masia, S. Micera, M. Akay, J.L. Pons (Eds.), Converging Clinical and Engineering Research on Neurorehabilitation III, Springer International Publishing, Cham, 2019, pp. 395–399.
[13] M. Totaro, T. Poliero, A. Mondini, C. Lucarotti, G. Cairoli, J. Ortiz, L. Beccai, Soft smart garments for lower limb joint position analysis, Sensors 17 (10) (2017) 2314, https://doi.org/10.3390/s17102314.
[14] B. Huang, M. Li, T. Mei, D. McCoul, S. Qin, Z. Zhao, J. Zhao, Wearable stretch sensors for motion measurement of the wrist joint based on dielectric elastomers, Sensors 17 (12) (2017) 2708, https://doi.org/10.3390/s17122708.
[15] L. Duan, D.R. D'hooge, L. Cardon, Recent Progress on flexible and stretchable piezoresistive strain sensors: from design to application, Prog. Mater. Sci. 114 (2020) 100617, https://doi.org/10.1016/j.pmatsci.2019.100617. November 2019.
[16] A. Atalay, V. Sanchez, O. Atalay, D.M. Vogt, F. Haufe, R.J. Wood, C.J. Walsh, Batch fabrication of customizable silicone-textile composite capacitive strain sensors for human motion tracking, Adv. Mater. Technol. 2 (9) (2017) 1700136, https://doi.org/10.1002/admt.201700136.
[17] Q. Zhang, Y.L. Wang, Y. Xia, P.F. Zhang, T.V. Kirk, X.D. Chen, Textile-only capacitive sensors for facile fabric integration without compromise of wearability, Adv. Mater. Technol. 4 (10) (2019) 1900485, https://doi.org/10.1002/admt.201900485.
[18] Y. Cao, T. Bu, C. Fang, C. Zhang, X. Huang, C. Zhang, High-resolution monolithic integrated tribotronic ingazno thin-film transistor array for tactile detection, Adv. Funct. Mater. 30 (35) (2020) 2002613, https://doi.org/10.1002/adfm.202002613.
[19] Y. Gao, L. Yu, J.C. Yeo, C.T. Lim, Flexible hybrid sensors for health monitoring: materials and mechanisms to render wearability, Adv. Mater. 32 (15) (2020) 1902133, https://doi.org/10.1002/adma.201902133.
[20] K. Xu, Y. Lu, K. Takei, Multifunctional skin-inspired flexible sensor systems for wearable electronics, Adv. Mater. Technol. 4 (3) (2019) 1800628, https://doi.org/10.1002/admt.201800628.
[21] R. Nur, N. Matsuhisa, Z. Jiang, M.O.G. Nayeem, T. Yokota, T. Someya, A highly sensitive capacitive-type strain sensor using wrinkled ultrathin gold films, Nano Lett. 18 (9) (2018) 5610–5617, https://doi.org/10.1021/acs.nanolett.8b02088.
[22] Q. Zhou, B. Ji, Y. Wei, B. Hu, Y. Gao, Q. Xu, J. Zhou, B. Zhou, A bio-inspired cilia array as the dielectric layer for flexible capacitive pressure sensors with high sensitivity and a broad detection range, J. Mater. Chem. A 7 (48) (2019) 27334–27346, https://doi.org/10.1039/C9TA10489E.
[23] J. Pignanelli, K. Schlingman, T.B. Carmichael, S. Rondeau-Gagné, M.J. Ahamed, A comparative analysis of capacitive-based flexible pdms pressure sensors, Sensors Actuators A Phys. 285 (2019) 427–436, https://doi.org/10.1016/j.sna.2018.11.014.
[24] X. Yang, Y. Wang, X. Qing, A flexible capacitive sensor based on the electrospun pvdf nanofiber membrane with carbon nanotubes, Sensors Actuators A Phys. 299 (2019), 111579, https://doi.org/10.1016/j.sna.2019.111579.
[25] C.C. Vu, J. Kim, Highly elastic capacitive pressure sensor based on smart textiles for full-range human motion monitoring, Sensors Actuators A Phys. 314 (2020), 112029, https://doi.org/10.1016/j.sna.2020.112029.
[26] S.H. Lee, H. Seo, S. Lee, Fabrication of a printed capacitive air-gap touch sensor, Jpn. J. Appl. Phys. 57 (5S) (2018) 05GC04, https://doi.org/10.7567/jjap.57.05gc04.
[27] O. Atalay, A. Atalay, J. Gafford, C. Walsh, A highly sensitive capacitive-based soft pressure sensor based on a conductive fabric and a microporous dielectric layer, Adv. Mater. Technol. 3 (1) (2018) 1700237, https://doi.org/10.1002/admt.201700237.
[28] Y. Luo, J. Shao, S. Chen, X. Chen, H. Tian, X. Li, L. Wang, D. Wang, B. Lu, Flexible capacitive pressure sensor enhanced by tilted micropillar arrays, ACS Appl. Mater. Interfaces 11 (19) (2019) 17796–17803, https://doi.org/10.1021/acsami.9b03718.
[29] S. Pyo, J. Choi, J. Kim, Flexible, transparent, sensitive, and crosstalk-free capacitive tactile sensor array based on graphene electrodes and air dielectric, Adv. Electr. Mater. 4 (1) (2018) 1700427, https://doi.org/10.1002/aelm.201700427.
[30] S.-Z. Guo, K. Qiu, F. Meng, S.H. Park, M.C. McAlpine, 3d printed stretchable tactile sensors, Adv. Mater. 29 (27) (2017) 1701218, https://doi.org/10.1002/adma.201701218.
[31] M.A. Butt, N.L. Kazanskiy, Revolution in flexible wearable electronics for temperature and pressure monitoring—a review, Electronics 11 (2022) 716, https://doi.org/10.3390/electronics11050716.
[32] TkInter - Python Wiki, URL, https://wiki.python.org/moin/TkInter, 2021.